

# SCIENTIFIC REPORTS



OPEN

## Lack of inflammatory gene expression in bats: a unique role for a transcription repressor

Arinjay Banerjee<sup>1</sup>, Noreen Rapin<sup>1</sup>, Trent Bollinger<sup>2</sup> & Vikram Misra<sup>1</sup>

In recent years viruses similar to those that appear to cause no overt disease in bats have spilled-over to humans and other species causing serious disease. Since pathology in such diseases is often attributed to an over-active inflammatory response, we tested the hypothesis that bat cells respond to stimulation of their receptors for viral ligands with a strong antiviral response, but unlike in human cells, the inflammatory response is not overtly activated. We compared the response of human and bat cells to poly(I:C), a viral double-stranded RNA surrogate. We measured transcripts for several inflammatory, interferon and interferon stimulated genes using quantitative real-time PCR and observed that human and bat cells both, when stimulated with poly(I:C), contained higher levels of transcripts for interferon beta than unstimulated cells. In contrast, only human cells expressed robust amount of RNA for TNF $\alpha$ , a cell signaling protein involved in systemic inflammation. We examined the bat TNF $\alpha$  promoter and found a potential repressor (c-Rel) binding motif. We demonstrated that c-Rel binds to the putative c-Rel motif in the promoter and knocking down c-Rel transcripts significantly increased basal levels of TNF $\alpha$  transcripts. Our results suggest bats may have a unique mechanism to suppress inflammatory pathology.

Bats are thought to be natural reservoirs for several emerging and re-emerging viruses such as those that closely resemble severe acute respiratory syndrome (SARS), Middle East respiratory syndrome (MERS) and porcine epidemic diarrhoea (PED) – causing coronaviruses (CoV), Marburg and, possibly, Ebola flaviviruses, and Hendra and Nipah paramyxoviruses, amongst others<sup>1–5</sup>. These viruses are speculated to have spilled over from bats to humans and other animals, directly or through intermediate hosts, causing severe and often fatal disease. Despite evidence of bats harbouring these viruses, or viruses closely related to them, bats do not appear to show overt symptoms or clinical signs of infection<sup>6</sup>. Infecting Pteropid, Jamaican and Egyptian fruit bats with Nipah and Hendra viruses, MERS-CoV and Ebolavirus yielded no evidence of disease. The bats sero-converted and in some cases virus could be detected post infection<sup>7–10</sup>, but these bats did not demonstrate signs of illness. We do not completely understand why bats are less susceptible to these viral infections than other mammals that often succumb.

The immune system, based on our knowledge from humans and other mammals, can be broadly categorised into two branches – the innate immune system and the adaptive immune system<sup>11</sup>. Both branches are distinct, although there is interaction between them. During viral infection, the innate response is the first line of defence and primes the adaptive immune response against the virus<sup>12, 13</sup>. A virus infected cell detects several pathogen associated molecular patterns (PAMPs) associated with the virus through pattern recognition receptors (PRRs) present in endosomal compartments, cytoplasm and cell membrane [reviewed by Mogensen<sup>14</sup>]. Some of these PRRs, such as toll-like receptors (TLRs) 3, 7, 8, 9, Retinoic acid-inducible gene I (RIG-I) and Melanoma Differentiation-Associated protein 5 (MDA5), have specifically evolved to recognise microbial nucleic acids [reviewed by Lee and Kim<sup>15</sup>]. Polyinosinic:polycytidylic acid [poly(I:C)] is a known double-stranded RNA analogue which is detected by TLR3, RIG-I and MDA5. After detection, PRRs signal through mediators to activate two pathways - the antiviral cytokine (interferons) and inflammatory pathways<sup>16</sup>.

Nuclear factor kappa-light-chain-enhancer of activated B cells (NF $\kappa$ B) and interferon regulatory factor 3 (IRF3) are two signal mediators that activate antiviral and inflammatory pathways in response to double-stranded RNA sensed by TLR3, RIG-I and MDA5 [reviewed by Mogensen<sup>14</sup>]. Five members of the NF $\kappa$ B family of proteins

<sup>1</sup>Department of Veterinary Microbiology, Western College of Veterinary Medicine, University of Saskatchewan, Saskatoon, Saskatchewan, S7N 5B4, Canada. <sup>2</sup>Department of Veterinary Pathology, Western College of Veterinary Medicine, University of Saskatchewan, Saskatoon, Saskatchewan, S7N 5B4, Canada. Correspondence and requests for materials should be addressed to V.M. (email: [vikram.misra@usask.ca](mailto:vikram.misra@usask.ca))

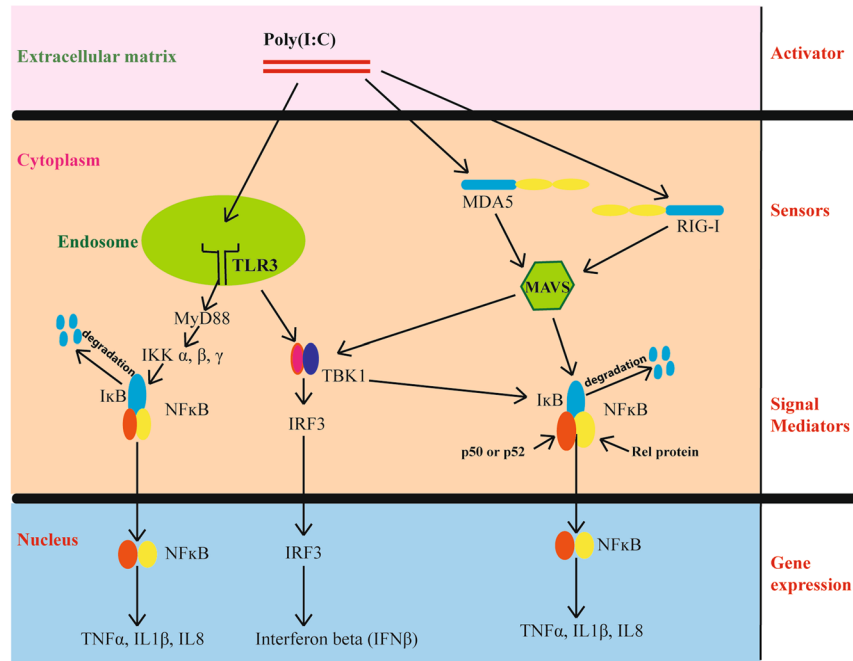


**Figure 1.** Schematic representation of detection of double-stranded RNA in a human cell and activation of the innate immune response. RNA viruses during replication produce double-stranded RNA intermediates (PAMPs), which are detected by cellular receptors (PRRs). Poly(I:C) is a known double-stranded RNA analogue (activator) which is detected by sensors such as TLR3 (black), RIG-I and MDA5 (blue, CARD domains in yellow) in a cell. These sensors, when stimulated by the activator, lead to the expression of interferons (IFN $\beta$ ) and inflammatory genes (TNF $\alpha$ , IL1 $\beta$ , IL8) through adaptor proteins (MAVS and MyD88) and signal mediators such as NF $\kappa$ B (orange and yellow subunits) and IRF3. NF $\kappa$ B is retained in an inactive state in the cytoplasm by inhibitory molecules such as I $\kappa$ B (blue). Upon receiving an activation signal via a sensor, kinases (TBK1) phosphorylate IRF3, which then translocates to the nucleus to activate transcription. Kinases, such as IKK  $\alpha$ ,  $\beta$  or  $\gamma$  phosphorylate I $\kappa$ B inhibitors and mark them for degradation, thereby activating NF $\kappa$ B. Active NF $\kappa$ B then causes expression of downstream genes by translocating to the nucleus.

have been identified in humans, namely, RelA (p65), RelB, c-Rel, NF $\kappa$ B-1 (p50) and NF $\kappa$ B-2 (p52). All five members form homo- or hetero-dimers and share some structural features. These dimers are bound by molecules of the inhibitor of NF $\kappa$ B (I $\kappa$ B) family and retained in the cytoplasm of the cell in an inactivated state. After PAMP recognition, downstream signals mark the inhibitors for degradation and the dimers translocate to the nucleus of the cell to cause expression of antiviral and inflammatory genes<sup>17</sup> (Fig. 1). Different combinations of the proteins have vastly different effects on gene expression<sup>18</sup>. For instance, hetero-dimers of p50 or p52 and p65 or RelB activate transcription. In contrast, c-Rel as a homo-dimer or in association with p50 or p65, represses transcriptional activation by NF $\kappa$ B<sup>19</sup>.

*Chiroptera* is a very diverse order and information about one genus or species may not apply to all bats. However, *Pteropus alecto* (black flying fox) is being extensively studied to better understand the bat immune system. Three and a half percent of *P. alecto* transcribed genes, amounting to about 500 genes, correspond to immune genes<sup>20</sup>. *P. alecto* homologs to human TLR 1–10 have been sequenced and TLR 13 has been described. RIG-I, major histocompatibility complex I (MHC-I) and interferon regulatory factor 7 (IRF7) have been detected and characterized<sup>21–23</sup>. The interferon pathway, immunoglobulins and the presence of microRNAs have been substantiated in this bat. Constitutive expression of interferon alpha and the ability of cells derived from *P. alecto* to mount an interferon beta (IFN $\beta$ ) response to viral challenges has been demonstrated<sup>24–30</sup>.

A robust antiviral and a controlled inflammatory response is desirable to control a viral infection. During SARS-CoV and MERS-CoV infection in humans and PED-CoV infection in pigs, the viruses inhibit an early interferon response and cause massive secretion of pro-inflammatory chemokines and cytokines, leading to excessive recruitment of immune cells<sup>31–33</sup>. This is detrimental as an excessive inflammatory response causes tissue damage and organ dysfunction in the host<sup>34</sup>.

In this study, we hypothesized that *Eptesicus fuscus* (big brown bat) cells would mount a strong antiviral cytokine response but a low inflammatory response to poly(I:C), synthetic single-stranded RNA (ssRNA, a viral single-stranded RNA surrogate), and CpG oligo deoxynucleotides (CpG ODN, a viral and bacterial DNA surrogate). These are known stimulants for human TLRs 3, 7/8 and 9 respectively. We compared the response of immortalized *E. fuscus* kidney cells (EfK3)<sup>35</sup> as well as *E. fuscus* bone marrow derived myeloid cells stimulated with poly(I:C) with that of human fibroblast cells (MRC5). We quantified the expression of innate response genes including IFN $\beta$ , tumor necrosis factor alpha (TNF $\alpha$ ), interleukin 8 (IL8) and others using quantitative real-time polymerase chain reaction (qRT-PCR). We observed that both bat and human cells mounted a strong

IFN $\beta$  response but only human cells expressed high levels of transcripts for proinflammatory cytokines such as TNF $\alpha$  and IL8 after TLR ligand treatments. To further explore the low TNF $\alpha$  response in bat cells, we analyzed the *E. fuscus* TNF $\alpha$  promoter for transcription factor binding motifs and identified a potential binding site for c-Rel proto-oncoprotein, a known suppressor of gene expression<sup>36</sup>. Ectopically expressed c-Rel bound to DNA containing this motif and the protein localized to the nucleus of bat cells in response to poly(I:C). Deletion of this motif in the promoter enhanced activation by poly(I:C) and partial knockdown of bat c-Rel RNA by specific small interfering RNA (siRNA) increased basal levels of TNF $\alpha$  transcripts in bat cells. We could detect c-Rel transcripts in every major big brown bat tissue, such as spleen, gut, ileum, kidney, lung, liver and the bat kidney cell line, unlike in humans, where it is found predominantly in hematopoietic cells<sup>37</sup>. Finally, we could also demonstrate that bat c-Rel bound to the potential motif as promoters containing the motif were co-immunoprecipitated to higher levels than promoters that lacked this motif. Our results suggest that bats might have evolved a unique mechanism to suppress an exaggerated inflammatory response to viruses.

## Results

**TLR expression in MRC5 and Efk3 cells.** To determine if the human and bat cell lines we studied expressed receptors for viral ligands, we examined these cells for TLR 2, 3, 7, 8, 9, RIG-I and MDA5 using PCR (see Supplementary Table S1). Both cell lines contained transcripts for these receptors.

**Big brown bat cells express high levels of IFN $\beta$  but low TNF $\alpha$  transcripts in response to poly(I:C).** To determine if the cells were capable of innate responses to viral ligands we treated the cells with poly(I:C), single-stranded RNA (ssRNA) and CpG ODNs. We used these surrogates instead of viruses capable of infecting both cells to prevent modulation of these pathways by viral proteins.

We quantified the expression of several transcription factors and downstream genes by qRT-PCR. We observed a heightened innate response with poly(I:C) in bat cells but not as much with ssRNA and CpG ODN (see Supplementary Table S2). We therefore decided to further analyse the cytokine response in bat and human cells to poly(I:C). While both MRC5 and Efk3 cells responded to poly(I:C) with a robust increase in IFN $\beta$  transcripts (Fig. 2a), only MRC5 cells responded with increased levels of TNF $\alpha$  RNA (Fig. 2b). Poly(I:C)-treated Efk3 cells contained, on an average, 2.4 fold more TNF $\alpha$  transcripts than mock-treated cells, as compared to a 315-fold increase in human cells (Fig. 2b). We therefore examined further the response of these two genes. To determine when IFN $\beta$  and TNF $\alpha$  transcripts are expressed following poly(I:C) treatment, we quantified IFN $\beta$  and TNF $\alpha$  transcripts in MRC5 and Efk3 cells at different times after poly(I:C) treatment. Both MRC5 and Efk3 cells showed highest IFN $\beta$  transcript levels at 9 h post-transfection (Fig. 2c). TNF $\alpha$  transcript levels were highest at 12 h post-transfection in MRC5 cells and there was relatively little expression in Efk3 cells (Fig. 2d). To rule out the possibility of Efk3 cells not being able to mount a TNF $\alpha$  response, we transfected bone marrow derived myeloid cells from big brown bat long bones with poly(I:C). The mixed population of cells (see Supplemental Fig. S1) demonstrated an average of 1700-fold increase in IFN $\beta$  transcripts but only 11-fold increase in TNF $\alpha$  transcripts (Fig. 2e) post stimulation.

**Poly(I:C) signals through TLR3 to activate IFN $\beta$  in Efk3 cells.** To determine if poly(I:C) signaled through an intracellular receptor we measured IFN $\beta$  transcripts in bat cells treated either with poly(I:C) added to the medium or poly(I:C) transfected in to bat cells. We compared both treatment types to mock-treated cells. Adding poly(I:C) to the cell culture medium did not increase IFN $\beta$  transcripts in bat cells (see Supplemental Fig. S2). To further identify the roles of TLR3, RIGI and MDA5, the three intracellular receptors for dsRNA recognition in bat cells, we partially knocked down these receptors using siRNA. siRNA specific to these receptors significantly reduced transcripts for TLR3, RIGI and MDA5 (Fig. 3a). Knocking down TLR3 transcripts significantly reduced IFN $\beta$  transcripts after poly(I:C) transfection (Fig. 3b). Although knocking down RIGI also led to a decrease in IFN $\beta$  transcripts post poly(I:C) transfection, it was not significant (Fig. 3b). Knocking down MDA5 did not have any effect on IFN $\beta$  transcript levels after poly(I:C) transfection in bat cells (Fig. 3b).

**Poly(I:C) treatment leads to the suppression of the big brown bat wildtype TNF $\alpha$  promoter activity.** To determine if the difference in the response of Efk3 and MRC5 cells was because of inherent features in their promoters for TNF $\alpha$ , we cloned the human TNF $\alpha$  promoter<sup>38</sup> and the corresponding region upstream of the big brown bat TNF $\alpha$  coding sequences in a plasmid with the reporter gene, chloramphenicol acetyltransferase (CAT). We transfected the plasmids in MRC5 and Efk3 cells and observed that the big brown bat TNF $\alpha$  promoter showed decreased activity post poly(I:C) challenge in both MRC5 and Efk3 cells (Fig. 4). In contrast, the human TNF $\alpha$  promoter showed increased activity in both Efk3 and MRC5 cells after poly(I:C) challenge (Fig. 4).

**Big brown bat TNF $\alpha$  promoter has a unique c-Rel binding site.** Since the big brown bat TNF $\alpha$  promoter showed decreased activity post poly(I:C) stimulation, we examined the human TNF $\alpha$  promoter and bat nucleotide sequence 1,200 bases upstream from the TNF $\alpha$  coding sequence for potential transcription factor binding motifs using the bioinformatics tool PROMO<sup>39</sup>. Both promoters contained motifs for binding NF $\kappa$ B although the big brown bat TNF $\alpha$  promoter had one less site. In addition, the bat promoter had a putative c-Rel binding motif (Fig. 5) not present in the human counterpart.

**c-Rel inhibits big brown bat wildtype TNF $\alpha$  promoter activity.** By analyzing the nucleotide sequence of the big brown bat TNF $\alpha$  promoter, we identified a potential c-Rel binding site. To identify the role of this binding motif in the big brown bat TNF $\alpha$  promoter, we deleted it (Fig. 6a) and observed the promoter's activity in response to poly(I:C) in bat cells. Deleting the c-Rel binding site in the big brown bat TNF $\alpha$  promoter increased the promoter activity in response to poly(I:C) (Fig. 6b). To further identify the role of c-Rel in repressing the bat

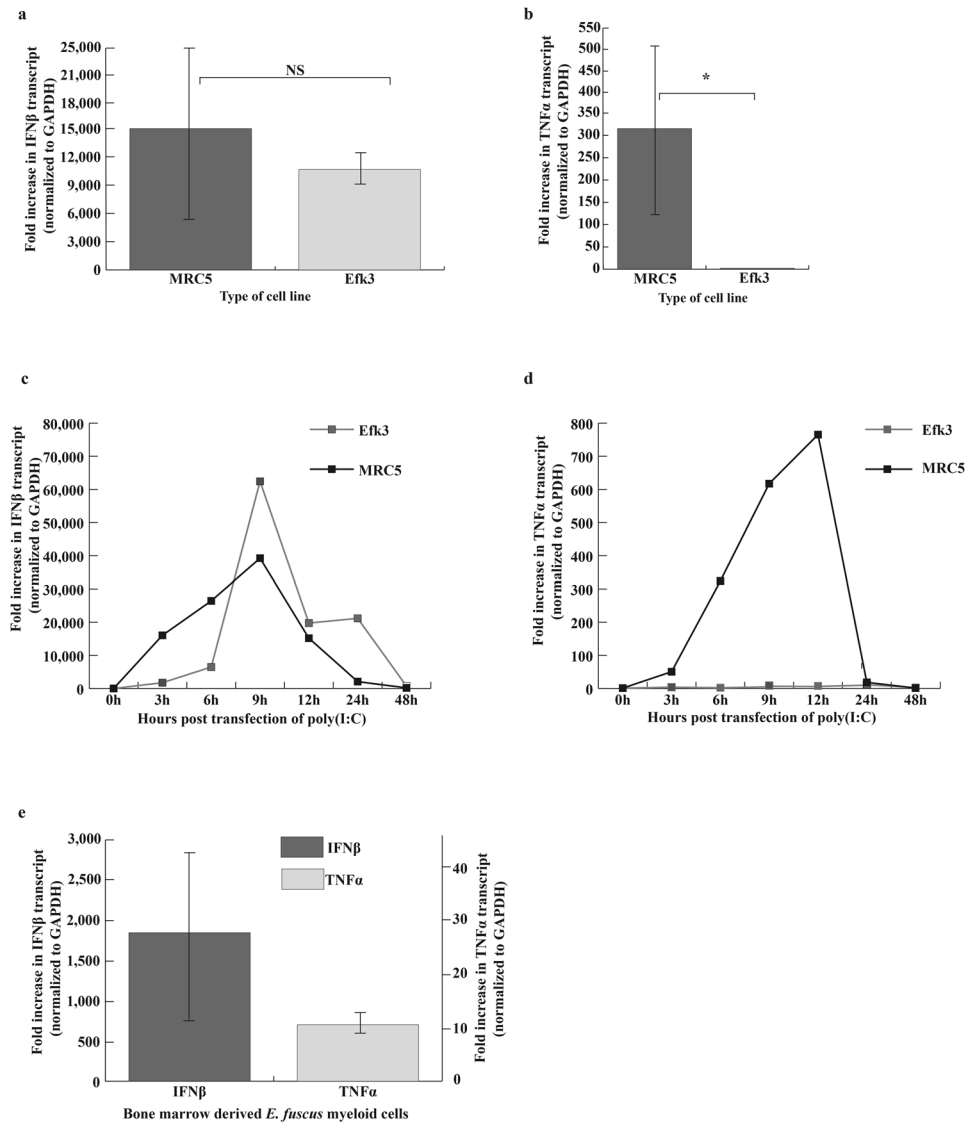


**Figure 2.** Efk3 cells do not express high levels of TNF $\alpha$  transcripts in response to poly(I:C). We transfected human fibroblasts, bat kidney (Efk3) and bat myeloid cells with poly(I:C), a known TLR3 stimulant, and studied the expression of IFN $\beta$  and TNF $\alpha$  relative to mock transfected cells. **(a)** Both MRC5 and Efk3 cells responded to poly(I:C) by expressing IFN $\beta$  transcripts (mean  $\pm$  SD,  $n = 3$ ,  $P = 0.05$ ). **(b)** MRC5 cells responded to poly(I:C) by several hundred fold expression of TNF $\alpha$  transcripts but Efk3 cells expressed significantly lower levels of TNF $\alpha$  transcripts (mean  $\pm$  SD,  $n = 3$ ,  $P = 0.021$ ). **(c)** Transcripts for IFN $\beta$  in MRC5 and Efk3 cells were quantified at several time points after poly(I:C) treatment. Both MRC5 and Efk3 cells showed highest IFN $\beta$  transcript levels 9 h post poly(I:C) treatment. **(d)** Transcripts for TNF $\alpha$  in MRC5 and Efk3 cells were quantified at several time points after poly(I:C) treatment. MRC5 cells showed highest TNF $\alpha$  transcripts 12 h post poly(I:C) treatment but Efk3 cells did not express TNF $\alpha$  transcripts to relatively comparable levels. **(e)** Big brown bat bone marrow derived myeloid cells expressed IFN $\beta$  transcripts to 1700 fold higher post poly(I:C) treatment but TNF $\alpha$  transcripts were expressed to an average of only 11 fold higher over mock treated cells (mean  $\pm$  SD,  $n = 3$ ). Results are expressed as fold increases over mock-treated cells normalized to GAPDH values (Materials and Methods). Statistical significance was calculated using two-tailed Mann-Whitney  $U$  test for two independent samples. \* $P < 0.05$ , NS = not significant.  $n$  is the number of independent experiments. SD = standard deviation.

TNF $\alpha$  promoter, we partially knocked down c-Rel transcripts using siRNA in bat cells (Fig. 6c) and quantified basal TNF $\alpha$  transcripts. There was a significant increase in basal TNF $\alpha$  transcripts in these cells (Fig. 6d). We further confirmed that siRNA directed against c-Rel used in this study could successfully shutdown the expression of c-Rel at a protein level (see Supplemental Fig. S3).

**Big brown bat c-Rel responds to poly(I:C) by translocating from the cytoplasm to the nucleus.** Rel proteins, either as hetero-dimers or homo-dimers, translocate to the nucleus of the cell after PAMP recognition and downstream signaling by PRRs to bind to promoters and regulate gene transcription. To

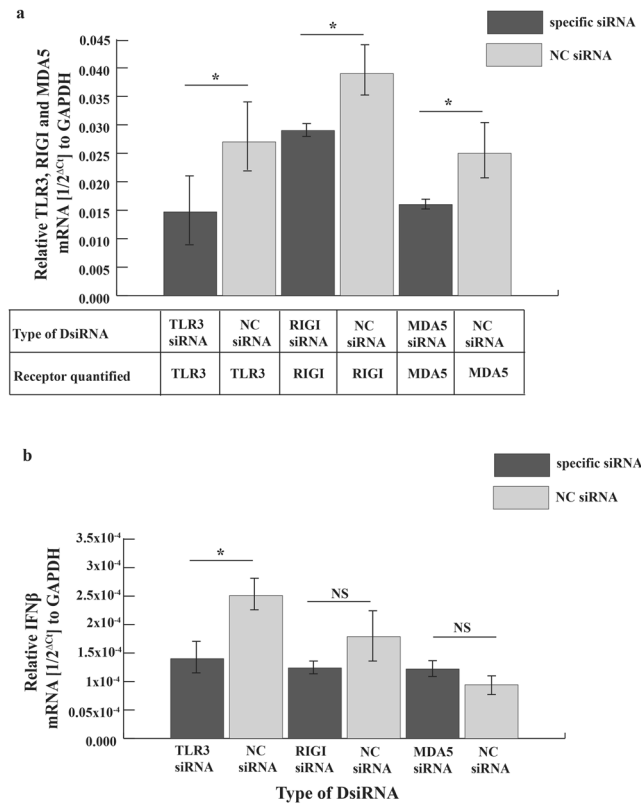


**Figure 3.** Poly(I:C) signals through TLR3 in Efk3 cells. To identify the role of TLR3, RIGI and MDA5 in poly(I:C) induced interferon signaling, we transfected siRNA specific to *E. fuscus* TLR3, RIGI or MDA5 in Efk3 cells and stimulated the cells with poly(I:C). **(a)** siRNA specific to these receptors partially knocked down transcripts for TLR3 ( $P = 0.043$ ), RIGI ( $P = 0.021$ ) and MDA5 ( $P = 0.02$ ) in poly(I:C) stimulated Efk3 cells (mean  $\pm$  SD,  $n = 4$ ). **(b)** Knocking down TLR3 in bat cells significantly reduced IFN $\beta$  transcripts after treatment with poly(I:C) (mean  $\pm$  SD,  $n = 4$ ;  $P = 0.02$ ). For cells in which RIGI transcripts had been specifically reduced by siRNA, the decrease in IFN $\beta$  transcripts was not significant (mean  $\pm$  SD,  $n = 4$ ;  $P = 0.05$ ). MDA5 knockdown did not correlate with decrease in IFN $\beta$  transcripts (mean  $\pm$  SD,  $n = 4$ ;  $P = 0.083$ ). Relative amounts of RNA are expressed as a reciprocal of Ct (the PCR cycle at which the product is measurable) normalized to Ct for GAPDH. Statistical significance was calculated using two-tailed Mann-Whitney  $U$  test for two independent samples. \* $P < 0.05$ , NS = not significant. NC = negative control.

determine if bat c-Rel responded to poly(I:C) treatment by similar movement, we cloned big brown bat c-Rel into a vector with an influenza virus haemagglutinin (HA) tag, that could be recognized by a commercially available monoclonal antibody, and transfected the protein expressing construct into Efk3 cells. We determined the cellular location of c-Rel by immunofluorescence and observed that c-Rel localized to the nucleus of poly(I:C) treated cells (Fig. 7a). In mock treated cells, c-Rel was present in the nucleus and the cytoplasm (Fig. 7a). The mean nuclear:cytoplasm fluorescence ratio was significantly higher in poly(I:C) treated cells than mock treated cells (Fig. 7b).

**Big brown bat c-Rel binds to the putative c-Rel binding site.** To study if bat c-Rel bound to the putative c-Rel motif, we co-transfected into human cells plasmids expressing HA-tagged bat c-Rel and plasmids containing wildtype or mutant bat and human TNF $\alpha$  promoters. We then performed chromatin immunoprecipitation (ChIP) assay on these cells using antibodies against the HA-tagged c-Rel. We used qRT-PCR to detect TNF $\alpha$  promoters in the immunoprecipitated samples. Bat c-Rel co-precipitated significantly higher amounts of big brown bat wildtype TNF $\alpha$  promoter with the putative c-Rel binding motif than the promoter without the motif (Fig. 8a). In addition, bat c-Rel precipitated a higher amount of the mutant human TNF $\alpha$  promoter with the putative bat c-Rel binding site than the wildtype human promoter (Fig. 8b).

## Discussion

*Chiroptera* is a very diverse order with over 1300 species of bats. Viruses from several families have been detected in different species of bats<sup>4</sup> although very few of these viruses are known to cause disease in their natural hosts. West Nile virus, Eptesipox virus, a novel group I coronavirus and American bat vesiculovirus have been detected in asymptomatic big brown bats<sup>4,40</sup>. We do not completely understand how bats and viruses coexist. Researchers are working to identify unique adaptations that might allow bats to coexist with these viruses<sup>5,41,42</sup>. Our results indicate that big brown bats may have evolved a unique mechanism to avoid an overblown inflammatory response to activation of the TLR3 pathway by viral ligands. This is in addition to other adaptations in bats currently being



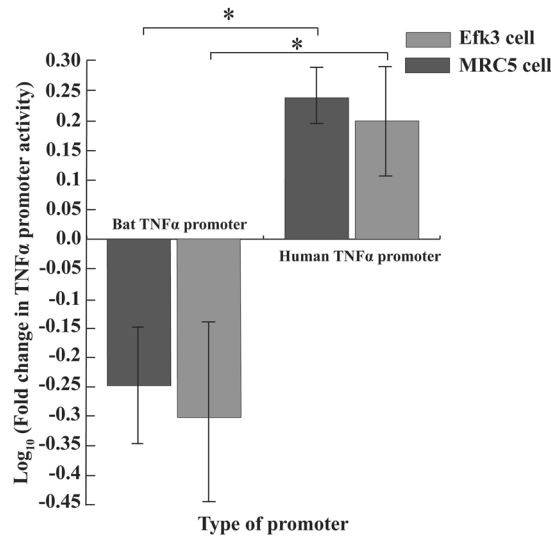


**Figure 4.** Big brown bat TNF $\alpha$  promoter is functionally different than its human counterpart. We transfected both human and bat TNF $\alpha$  promoters individually in human and bat cells and quantified their activity after poly(I:C) treatment by measuring the expression of a downstream surrogate gene, chloramphenicol acetyltransferase (CAT). Human TNF $\alpha$  promoter showed increased activity after poly(I:C) treatment (as measured by CAT activity) in both Efk3 ( $P = 0.021$ ) and MRC5 ( $P = 0.020$ ) cells. In contrast, big brown bat TNF $\alpha$  promoter showed decreased activity after poly(I:C) treatment in both Efk3 ( $P = 0.021$ ) and MRC5 ( $P = 0.020$ ) cells (mean  $\pm$  SD,  $n = 4$ ). Results are expressed as fold increases over mock-treated cells normalized to  $\beta$ -galactosidase. Statistical significance was calculated using two-tailed Mann-Whitney  $U$  test for two independent samples. \* $P < 0.05$ .



**Figure 5.** Big brown bat TNF $\alpha$  promoter has a unique c-Rel motif. Human and big brown bat TNF $\alpha$  promoters were analyzed for NF $\kappa$ B and c-Rel transcription factor binding sites. Human TNF $\alpha$  promoter has three NF $\kappa$ B binding and no c-Rel binding site. Big brown bat TNF $\alpha$  promoter has two NF $\kappa$ B binding site and one c-Rel binding site. Other transcription factor binding sites, including sites for NF $\kappa$ B-1 and Rel-A, are not shown here.

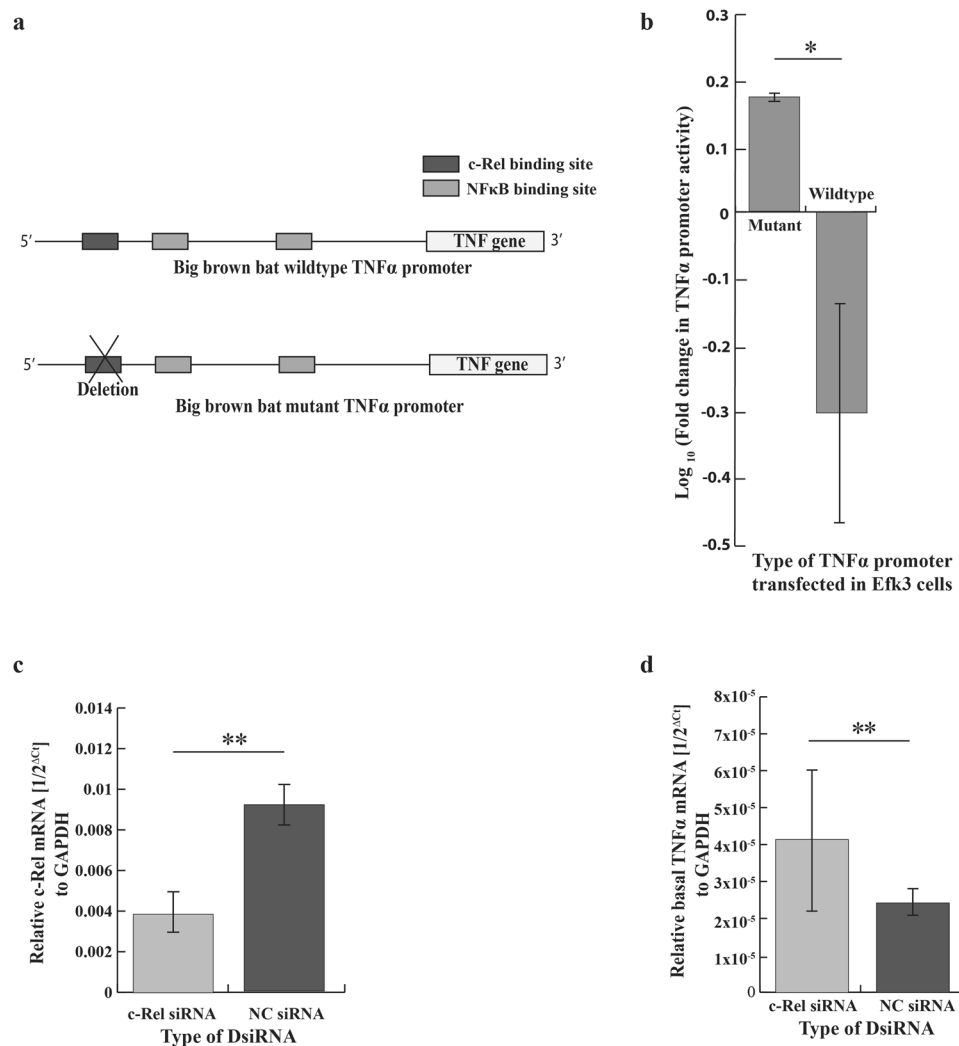


**Figure 6.** c-Rel acts as a repressor of the big brown bat TNF $\alpha$  promoter. **(a)** Schematic representation of big brown bat TNF $\alpha$  wildtype and mutant promoter. In the mutant bat promoter, the putative c-Rel binding site was deleted. **(b)** Deleting the putative c-Rel binding site in the wildtype big brown bat TNF $\alpha$  promoter significantly ( $P = 0.034$ ) increased the promoter activity in response to poly(I:C) treatment (mean  $\pm$  SD,  $n = 3$ ). **(c)** DsiRNA directed against bat c-Rel significantly ( $P = 0.009$ ) reduced c-Rel transcripts in bat cells (mean  $\pm$  SD,  $n = 5$ ). **(d)** Basal TNF $\alpha$  transcript levels increased significantly ( $P = 0.009$ ) in partially c-Rel knocked down bat cells (mean  $\pm$  SD,  $n = 5$ ). For Fig. 5C and D, relative amounts of RNA are expressed as a reciprocal of Ct (the PCR cycle at which the product is measurable) normalized to Ct for GAPDH. Statistical significance was calculated using two-tailed Mann-Whitney  $U$  test for two independent samples. \* $P < 0.05$ , \*\* $P < 0.01$ . NC = negative control.

proposed, such as loss of the PYHIN family of genes, thereby losing the ability to sense foreign DNA in cells and activating inflammasomes<sup>43</sup>.

To compare the innate responses of human and bat cells to viral ligands we treated the cells with surrogates of viral PAMPs. We used these surrogates instead of viruses capable of infecting both cells to prevent modulation of these pathways by viral proteins. In preliminary experiments we had determined that PED-CoV, which replicates and produces cytopathic effects in bat cells<sup>35</sup> does not induce an interferon response (data not shown). Coronavirus N protein is known to inhibit IFN $\beta$  production by preventing IRF3 phosphorylation<sup>44,45</sup>.

We observed an increase in IFN $\beta$  transcripts in Efk3 cells in response to poly(I:C), as has been previously demonstrated for other bat species<sup>46–48</sup>, but very little increase in TNF $\alpha$  transcripts compared to human cells. Recently, a *P. alecto* adaptive immune cell population was characterized and a subset of cells was shown to produce TNF $\alpha$  on stimulation with ionomycin, although the amount of TNF $\alpha$  produced was not reported<sup>49</sup>. We challenged big brown bat bone marrow derived myeloid cells and the kidney cell line with poly(I:C) and quantified the transcripts for representative antiviral and inflammatory genes. Inflammatory cytokine transcripts for TNF $\alpha$ , IL8 and IL1 $\beta$  (see Supplementary Table S2) in Efk3 cells and TNF $\alpha$  in big brown bat bone marrow derived myeloid cells were not expressed to levels observed in MRC5 cells. IFN $\beta$  and TNF $\alpha$  transcript levels observed in

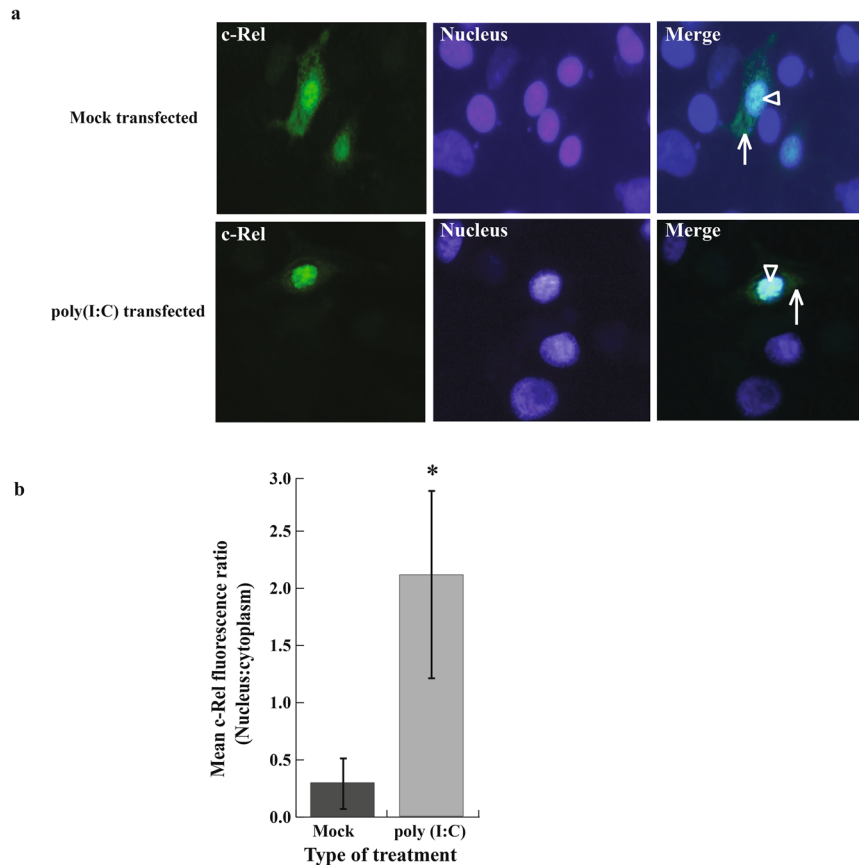


**Figure 7.** Big brown bat c-Rel localizes in the cell nucleus after poly(I:C) treatment. To characterize the bat c-Rel, we studied the cellular location of ectopically expressed c-Rel in poly(I:C) and mock transfected cells. **(a)** Big brown bat c-Rel localized primarily in the nucleus after poly(I:C) challenge compared to mock challenged cells, where ectopically expressed c-Rel localized both in the cytoplasm and nucleus. **(b)** Mean fluorescence ratio (i.e. nucleus:cytoplasm) was significantly ( $P = 0.021$ ) higher in poly(I:C) treated cells than mock treated cells (mean  $\pm$  SD,  $n = 4$ ). Statistical difference was calculated using two-tailed Mann Whitney  $U$  test for two independent samples.  $*P < 0.05$ .

poly(I:C) challenged big brown bat myeloid cells were comparable to levels observed in poly(I:C) challenged *P. alecto* bone marrow derived dendritic cells by Zhou *et al.*<sup>50</sup>

Interferon  $\beta$  production in response to poly(I:C) has been studied in bat cells<sup>35,47</sup> but the receptors involved in double-stranded RNA signaling have not been fully explored. Adding poly(I:C) to the culture medium did not upregulate transcripts for IFN $\beta$  in bat cells (see Supplemental Fig. S2) suggesting that the receptor recognizing poly(I:C) was intracellular. The requirement of transfection for the activation of TLR3 in certain cell types is supported by Zhou *et al.*<sup>51</sup>. Using siRNA, we were able to show for the first time that poly(I:C), and likely dsRNA, is recognized primarily through TLR3 in bat cells (Fig. 3). However, according to our results the role of RIGI in dsRNA recognition cannot be completely ruled out. The role of other PRRs in bats in recognizing specific ligands is yet to be explored.

TNF $\alpha$  plays a key role in inflammatory, infectious and malignant conditions. TNF $\alpha$  signaling transduction pathways are complex and are not fully understood<sup>52</sup>. NF $\kappa$ B plays a central role in the regulation of TNF $\alpha$  gene expression. Different combinations of the subunits that make up NF $\kappa$ B have vastly different effects on gene expression<sup>18</sup>. For instance, hetero-dimers of p50 or p52 and p65 or RelB activate transcription. In contrast, c-Rel as a homo-dimer or in association with p50 and p65, repress transcriptional activation by NF $\kappa$ B<sup>19</sup> and c-Rel has been previously shown to be a repressor of certain gene promoters in human cells, such as Ephrin type-B receptor 2 (EPHB2) in colorectal cancer cells<sup>36</sup>. We detected a putative c-Rel binding motif in the big brown bat TNF $\alpha$  promoter. Deleting this motif reversed the bat promoter activity after poly(I:C) treatment and partial knockdown of c-Rel RNA significantly increased basal TNF $\alpha$  transcript levels in bat cells demonstrating the ability of c-Rel to repress the TNF $\alpha$  promoter in bat cells.

The big brown bat TNF $\alpha$  promoter had two NF $\kappa$ B binding sites, which is one less than the human counterpart. We do not know if having one less NF $\kappa$ B binding site can be an additional reason for the low TNF $\alpha$  promoter activity. However, adding an additional NF $\kappa$ B binding site to the big brown bat promoter lacking the c-Rel binding site did not cause any further increase in promoter activity after poly(I:C) treatment (data not shown).



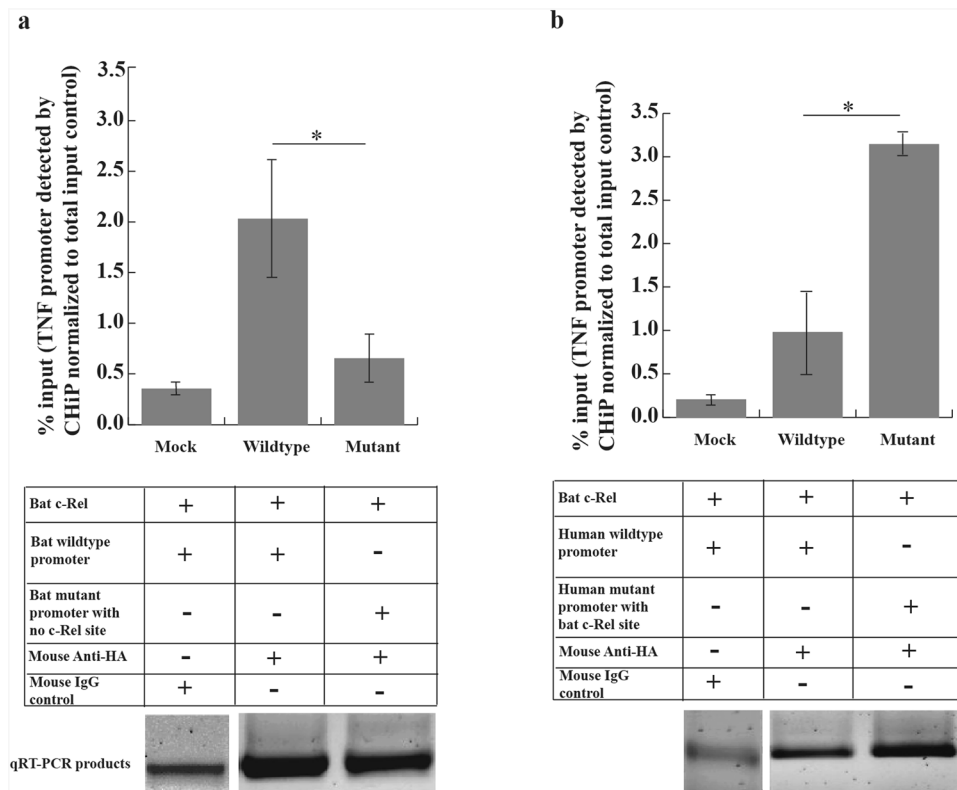


**Figure 8.** Big brown bat *c-Rel* binds to the putative *c-Rel* binding site. We co-transfected plasmids expressing HA-tagged bat *c-Rel* and human/bat  $\text{TNF}\alpha$  wildtype/mutant promoters in HEK293T cells. We immunoprecipitated *c-Rel* using HA-specific antibodies and quantified the amount of  $\text{TNF}\alpha$  promoter pulled down by qRT-PCR. **(a)** Bat *c-Rel* pulled down a significantly ( $P = 0.021$ ) higher amount of wildtype big brown bat  $\text{TNF}\alpha$  promoter that contained the putative *c-Rel* binding motif over the mutant promoter in which the motif was deleted (mean  $\pm$  SD,  $n = 4$ ). **(b)** Bat *c-Rel* pulled down a significantly ( $P = 0.021$ ) higher amount of mutant human  $\text{TNF}\alpha$  promoter which contained the putative bat *c-Rel* binding motif over the human wildtype  $\text{TNF}\alpha$  promoter, which lacked the *c-Rel* binding motif (mean  $\pm$  SD,  $n = 4$ ). qRT-PCR products obtained from quantifying the immunoprecipitated samples were electrophoresed on a gel and their representative cropped images are shown. Full length gel images are shown in Supplemental Fig. S5. Images have been acquired from two different gels. Statistical difference was calculated using two-tailed Mann Whitney  $U$  test for two independent samples  $*P < 0.05$ .

*c-Rel* might not be the only regulator of inflammatory gene expression and big brown bats may have evolved more than one mechanism to regulate inflammatory responses. We evaluated a second inflammatory gene,  $\text{IL1}\beta$  and found that it, like  $\text{TNF}\alpha$ , did not respond to poly(I:C) in bat cells (see Supplementary Table S2). However, while the  $\text{IL1}\beta$  promoter had identifiable  $\text{NF}\kappa\text{B}$  binding sites, it did not have a specific *c-Rel* binding site (data not shown). There is evidence that  $\text{NF}\kappa\text{B}$  molecules comprising p50 homodimers can act as transcriptional repressors (reviewed by Rothwarf and Karin<sup>53</sup>). Further work is required to identify the role of p50 homodimers in bat cells.

Zhang *et al.* have reported *c-Rel* to be under positive selection in bats based on whole-genome analysis of two distantly related species, fruit bat *P. alecto* and insectivorous bat *Myotis davidii*<sup>54</sup>. They suggest that the selection may have been driven by the involvement of *c-Rel* in DNA repair pathways and the need for efficient repair of damage caused by reactive oxygen species generated during flight. In addition, Enchéry and Horvat have also speculated that the positive selection of *c-Rel* may contribute to bats' immunovirological peculiarities<sup>55</sup>. Our results suggest that the positive selection of *c-Rel* may also have been driven by the need to dampen the destructive effects of inflammation in response to viral infections. Zhang *et al.* also identified mutations in the REL homology domain (RHD) of *c-Rel* that could potentially affect the binding of  $\text{I}\kappa\text{B}$  and speculated that this may allow nuclear transport in the absence of TLR3 stimulation<sup>54</sup>. These mutations are also present in big brown bat *c-Rel* (see Supplementary Fig. S4). However, we did find that while ectopically expressed bat *c-Rel* was present in both cytoplasm and nucleus, poly(I:C) stimulation increased translocation to the nucleus (Fig. 7a). The mutations, therefore, do not completely obviate TLR3 control.

We have also shown that big brown bat *c-Rel* physically interacts with the putative *c-Rel* binding site. Promoters containing the putative *c-Rel* binding site were co-immunoprecipitated at higher levels by the bat *c-Rel* than promoters that lacked it (Fig. 8). These results demonstrate that bat *c-Rel* can suppress the expression of  $\text{TNF}\alpha$  and that its putative binding site in the promoter for the gene plays a role. However, we have not identified

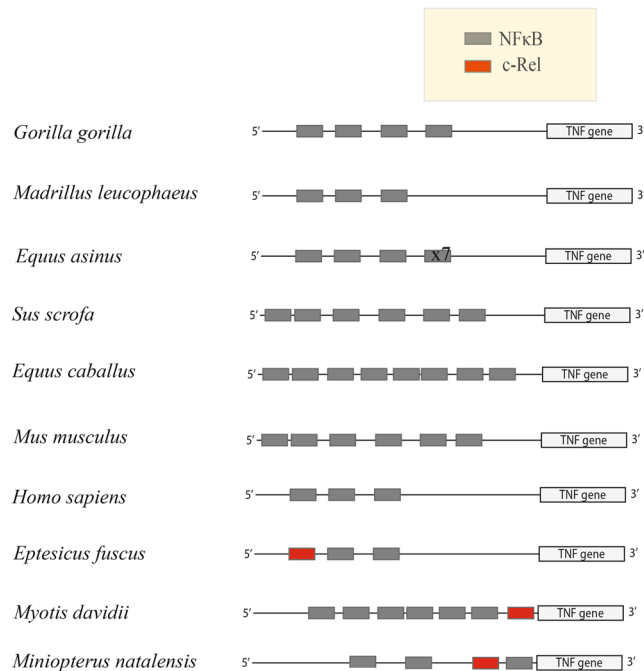


**Figure 9.** Bats are unique in having c-Rel binding sites in their TNF $\alpha$  promoter. At least three species of bats, *E. fuscus*, *M. davidii* and *M. natalensis* have c-Rel binding sites upstream of the TNF $\alpha$  gene. c-Rel sites (red boxes) are absent in the 1000 bp region upstream of the TNF $\alpha$  gene in other mammals represented in this figure. The number of NF $\kappa$ B binding motifs (gray boxes) in the TNF $\alpha$  promoter varied amongst mammals. All sites were predicted using PROMO. For *Equus asinus* x7 indicates 7 additional copies of the NF $\kappa$ B binding site.

the mechanism by which c-Rel acts. More work is also needed to characterize the interaction between the various NF $\kappa$ B subunits and their downstream effects on different promoters.

Proteins of the Rel family differ according to tissue types in humans. Rel family protein, p65 is found in virtually all cell types, whereas c-Rel complexes (eg. p50/c-Rel and c-Rel homo-dimers) are predominantly expressed in cells of hematopoietic lineage, such as lymphoid and myeloid cells<sup>37</sup>. We detected c-Rel transcripts in a wide variety of big brown bat tissues such as spleen, gut, ileum, kidney, lung, liver and the kidney cell line (Efk3) as well (see Supplementary Table S3). We further analysed the promoters of animals in different mammalian orders and could not detect a c-Rel binding motif in the sequence 1000 bp upstream of their TNF $\alpha$  genes. We detected potential c-Rel binding sites in other bats such as *M. davidii* and *M. natalensis* (Fig. 9). We did not detect a potential c-Rel binding site in the *P. alecto* DNA sequences that lie upstream from the TNF $\alpha$  coding sequences but there was one downstream of the coding sequences (data not shown). The potential role of c-Rel in the DNA repair pathway and evolution of flight in bats has been proposed by Zhang *et al.*<sup>54</sup>. We do not yet fully understand the role of c-Rel in DNA repair pathways in different tissue types in bats and in different species of bats. Different bat species could have evolved different strategies or a combination of strategies to control an overblown inflammatory response.

Our study demonstrates that big brown bats have possibly evolved a mechanism to control the over expression of inflammatory genes in response to activation of their innate immune system by viral nucleic acid PAMPS. Our work raises several questions about the bat innate immune response that need to be further explored. Identifying unique defence mechanisms in bats might allow us to extend the knowledge for therapeutic purposes in spill-over hosts that often develop significant disease or succumb to infections with these viruses.

## Materials and Methods

**Ethics statement.** Long bones (femur and humerus) and organs were obtained from big brown bats submitted to Canadian Wildlife Health Cooperative (CWHC). The bats were euthanized by a protocol approved by the Committee on Animal Care and Supply of the University of Saskatchewan Animal Research Ethics Board (protocol #20090036) and were in accordance with regulations approved by the Canadian Council on Animal Care.

**Cell culture.** *Eptesicus fuscus* kidney cells (Efk3) were grown in Dulbecco's Minimal Essential Medium with GlutaGro (DMEM; Corning) containing 10% fetal bovine serum (FBS; Seradigm), Penicillin/Streptomycin (Gibco) and 1% GlutaMax (Gibco). MRC5 cells (ATCC CCL-171) were cultured in Minimum Essential Medium Eagle (MEM; Corning) supplemented with 10% FBS, 1/100 non-essential amino acids (NEAA; Gibco), 1/100 4-(2-hydroxyethyl)-1-piperazineethanesulfonic acid (HEPES; Gibco) and 1/1000 gentamycin (Gibco). HEK293T cells (Dr. Robert Brownlie, VIDO-Intervac) were cultured in DMEM with GlutaGro containing 10% FBS and Penicillin/Streptomycin. For bone marrow derived myeloid cells, bone marrow from big brown bat long bones was processed as described for mice<sup>56</sup>. The cells were seeded in Roswell Park Memorial Institute

Sequence	Primers	Features and legend
Human TNF alpha promoter	GCCGGTACCGCTGTCTGCTGTGTGTGTG and GCCCTCGAGGGGACACACAAGCATCAAG	KpnI and XhoI sites
Big brown bat TNF alpha promoter	GCCACGCGTAAGAATGTCTCGGGCTGTT and GCCCTCGAGGCTGTGTCTCCAGAGGCC	MluI and XhoI sites
Big brown bat cRel CDS cloned in pCMV-HA-N	GCCGTCGACCATGCGTTTTTCGATACAAATG and GCCCGCGCCGCTTACAAGTTAACCGGAAAAA	SalI and NotI sites
CD.Ri.17417.13.1 (cRel_siRNA) - sequence	rArArA rGrGrA rArGrC rUrArU rUrArU rUrUrC rArArG rArATA	r = ribose sugar
CD.Ri.17417.13.1 (cRel_siRNA) - sequence2	rUrArU rUrCrU rUrGrA rArArU rArArU rArGrC rUrUrC rCrUrU rUrArC	r = ribose sugar
CD.Ri.17417.13.2 (cRel_siRNA) - sequence	rGrGrA rArGrA rUrUrC rArUrU rArArA rArArA rGrArA rUrCA A	r = ribose sugar
CD.Ri.17417.13.2 (cRel_siRNA) - sequence2	rUrUrG rArUrU rCrUrU rUrUrU rUrArA rUrGrA rArUrC rUrUrC rCrUrU	r = ribose sugar
Big brown bat TNF alpha promoter - ChIP primers	GGCAGATGTGGCCACAGGCAGAG and CAGAGAGCTGAGTCCTTGACG	—
Human TNF alpha promoter - ChIP primers	GGGGAGAACAAAAGGATAAGG and CTCTCACTTCTCAGGCCCCAG	—

**Table 1.** siRNA, cloning and ChIP qRT-PCR primer sequences. For siRNA sequences, ribonucleotides are preceded by the letter ‘r’. Cloning primer sequences contain restriction sites as part of the sequence.

1640 (RPMI; Sigma-Aldrich) medium containing 10% FBS, Penicillin/Streptomycin and 20 ng/ml human granulocyte-macrophage colony-stimulating factor (hGM-CSF; PeproTech).

**TLR challenge.** MRC5, Efk3 and big brown bat bone marrow derived myeloid cells were seeded at a concentration of  $3 \times 10^5$  cells/well in 6 well plates and transfected with TLR ligands. Briefly, cell lines were transfected with 750 ng/ml poly(I:C) (InvivoGen) or 4 µg/ml single-stranded RNA 40 (ssRNA40; InvivoGen) or 3 µM CpG ODN (InvivoGen) using Lipofectamine 2000 (Invitrogen). Cells were harvested 16 h post-transfection and RNA was extracted. For time-point experiments, cell lines were treated with the above-mentioned concentrations of TLR ligands and RNA was extracted at indicated time points.

**Nucleic acid extraction, PCR and qRT-PCR.** All RNA extractions were performed using the RNeasy Plus Mini kit (QIAGEN, Germany) as per manufacturer’s instructions. cDNA was prepared using the QuantiTect Reverse Transcription kit (QIAGEN) as per manufacturer’s instructions. One µg of RNA was used for cDNA preparation. cDNA was used as a template for the quantification of target genes. DNA extraction from MRC5 and Efk3 cells was performed using the DNeasy Blood and Tissue kit (QIAGEN) as per manufacturer’s instructions.

Conventional PCR was performed to amplify human or big brown bat TNF $\alpha$  promoters, big brown bat c-Rel coding sequence (CDS) and cDNA from c-Rel transcripts in big brown bat organs using specific primers. Primers with restriction sites were used to clone the TNF $\alpha$  promoters and c-Rel CDS (Table 1). Primers without restriction sites were designed to detect c-Rel transcripts in big brown bat organs (see Supplementary Table S4). Human TNF $\alpha$  promoter sequence was obtained from NCBI (Accession number: AB048818) and amplified by PCR from DNA extracted from MRC5 cells. The big brown bat TNF $\alpha$  promoter was defined as a sequence up to 1200 bp upstream of the TNF $\alpha$  gene (sequence submitted; GenBank accession: BK009991) and amplified by PCR from DNA extracted from Efk3 cells. Big brown bat c-Rel sequence was obtained from NCBI (Accession number: XM\_008162099.1). PCR was performed using the following thermal cycle profile: initial denaturation for 3 min at 94 °C, 35 PCR cycles at 94 °C/30 s, 55 °C/30 s and 72 °C/1 min. The final extension was at 72 °C for 10 min.

For the quantification of innate immune response genes, qRT-PCR assays targeting respective gene transcripts (see Supplementary Table S4) and the normalizer (Glyceraldehyde-3-phosphate; GAPDH) were performed for both MRC5 and Efk3 cells. Agilent’s MX3005P PCR cyclor was used in conjunction with Quantifast SYBR Green PCR kit (QIAGEN) and samples were prepared as previously mentioned<sup>37</sup>. Primers for Efk3 cells were designed using the annotated big brown bat genome (Accession No. PRJNA72449). Primer sequences for MRC5 cells were obtained from PrimerBank<sup>58, 59</sup> or nucleotide database on National Centre for Biotechnology Information (NCBI). When primer sequences were not available for MRC5 or genes not annotated for big brown bat, multiple sequence alignment was performed with other mammalian homologues and primers were designed against conserved regions. One of the cytokines, IL8, is not annotated in the big brown bat genome. Primers for IL8 were designed using the annotated *Myotis lucifugus* genome. The products were quantified based on the amount of relative gene expression. All amplified products were confirmed on a gel and sequenced (Macrogen). Reaction efficiencies for qRT-PCR primers were between 95 and 105%.

For qRT-PCR, after the initial denaturation step of 95 °C for 5 minutes, two step cycling for 40 cycles was performed at 95 °C/10 s, (51–56) °C/30 s. Absorbance readings were acquired after each cycle. The final three steps were carried out at 95 °C/1 min, 55 °C/30 s and 95 °C/30 s to generate the dissociation curve. Absorbance readings for the dissociation curve were acquired at every degree from 55–95 °C. The annealing temperatures were optimized for different groups of genes (see Supplementary Table S4). Relative fold change in gene expression between the two groups of cells (treated and mock treated) was calculated after normalizing the Ct values using GAPDH. Three housekeeping genes were tested (GAPDH,  $\beta$ -actin and  $\beta$ -2-microglobulin) for MRC5 and two for Efk3 cells (GAPDH and  $\beta$ -actin). There was no variation in Ct values for the housekeeping genes between treated

and mock treated samples. Thus GAPDH was chosen for normalizing the data. Difference of one Ct indicates a two-fold difference in gene expression.

qRT-PCR for quantifying immunoprecipitated DNA after the ChIP assay was performed using primers (Table 1) designed to amplify a region spanning the putative c-Rel binding site of approximately 480 bp for the bat promoter and 410 bp for the human promoter ( $\pm$  the putative c-Rel binding motif). The reaction conditions were as described above.

**Agarose Gel Electrophoresis.** One percent agarose (Invitrogen, USA) gels were prepared using 0.5X TBE [Tris – 1 M (VWR), Ethylenediaminetetraacetic acid disodium salt (EDTA) solution – 0.02 M (Gibco) and Boric acid – 1 M; pH 8.4]. One  $\mu$ l SYBR Safe DNA gel stain (Invitrogen) was added for every 1 ml of gel. Ten  $\mu$ l of PCR or qRT-PCR products were run on the gel for 1 h at 105 volts and visualized under an ultraviolet gel imaging system (AlphaImager HP).

**Cloning TNF $\alpha$  promoter and c-Rel.** Human TNF $\alpha$  promoter sequence was amplified by PCR from DNA extracted from MRC5 cells and cloned in pCAT3 vector (Promega) upstream of the chloramphenicol acetyltransferase (CAT) gene using restriction sites KpnI and XhoI. The big brown bat TNF $\alpha$  promoter was amplified by PCR using DNA extracted from Efk3 cells and cloned upstream of the CAT gene in a pCAT3 vector using restriction sites MluI and XhoI. Big brown bat c-Rel coding sequence (CDS) was amplified from cDNA prepared from RNA extracted from Efk3 cells and cloned in-phase downstream of a Hemagglutinin (HA) tag in pCMV-HA-N vector (Clontech) using restriction sites Sall and NotI.

**Generating TNF $\alpha$  promoter mutants.** Mutant big brown bat and human TNF $\alpha$  promoters were generated by removing or adding the c-Rel binding site. Agilent's QuikChange II Site-Directed Mutagenesis kit was used as per a modification of the manufacturer's protocol suggested by Wang and Malcolm<sup>60</sup>. For the bat mutant promoter, two primers (IDT) were designed to loop out the c-Rel binding site, BBB M1 – F – GCTTCATACAAAACTGCCTTTGGATCCAAG and BBB M1 – R – CTTGGATCCAAAGGCAGTTTTTGTATGAAGC. The primers were used to amplify wild-type big brown bat TNF $\alpha$  promoter. For the human mutant promoter, primers were designed containing the putative bat c-Rel binding motif: Hu-M1-F- GAATGGGTTACAGGAGGGGCTTCGGATCCTCTGGGGAGATG and Hu-M1-R- CATCTCCCCAGAGGATCCGAAGCCCCTCCTGTAACCCATTC. The primers were used to amplify wild-type human TNF $\alpha$  promoter. Deletion and addition of the c-Rel binding site were confirmed by sequencing (Macrogen).

**Chloramphenicol acetyl transferase (CAT) and  $\beta$ -galactosidase ( $\beta$ -gal) assay.** MRC5 and Efk3 cells were seeded at a concentration of  $3 \times 10^5$  cells/well in 6 well plates. At 60–80% confluency, 500 ng of human or big brown bat TNF $\alpha$  promoter (wildtype or mutant), 500 ng  $\beta$ -galactosidase ( $\beta$ -gal) expressing plasmid and 1  $\mu$ g of pcDNA empty plasmid to make up a total of 2  $\mu$ g DNA/well was transfected using Lipofectamine 2000. After 24 h, the medium was replaced with fresh complete medium (DMEM). After 4 h, cell lines were transfected with 750 ng/ml poly(I:C) and incubated for 16 h. CAT and  $\beta$ -gal assays were performed as previously mentioned<sup>61</sup>.

**Partial knock-down of c-Rel, TLR3, RIGI and MDA5 transcripts in Efk3 cells.** Dicer-ready siRNA (DsiRNA) specific to big brown bat c-Rel, TLR3, RIGI and MDA5 were designed and obtained through Integrated DNA Technologies (IDT). A 100 nM final concentration of a 1:1 mixture of two DsiRNAs (Table 1 and see Supplementary Table S5) targeting separate regions on the respective transcript was transfected into Efk3 cells using Lipofectamine 2000. Scrambled non-specific DsiRNA (NC DsiRNA; IDT) was used as a negative control. Cy3 labelled DsiRNA (IDT) was used to confirm 100% transfection efficiency.

**Immunofluorescence.** Efk3 cells were seeded at a concentration of  $3 \times 10^5$  cells/well in 6 well plates with glass cover-slips and transfected with 5  $\mu$ g/well pCMV-HA-N plasmid expressing big brown bat c-Rel using Lipofectamine 2000. Cells were treated with 750 ng/ml poly(I:C) after 24 h and incubated for another 16 h. Media was discarded and cells were rinsed with 2 ml PBS. Cover-slips were transferred to wells containing ice-cold methanol in 6-well plates and incubated for 20 mins in a freezer. Methanol was discarded and cells were washed with PBS. Cells were blocked using a blocking solution [PBS, 10% newborn calf serum (Invitrogen) and 0.1% Tween 20 (USB)]. Primary staining for c-Rel was performed using 1:2000 dilution (as used by Smith *et al.*<sup>62</sup>) of mouse anti-HA (Sigma). Secondary staining was performed using 4  $\mu$ g/ml goat anti-mouse Alexa 488 (Molecular Probes) and 0.2  $\mu$ g/ml Hoechst 33342 (Molecular Probes) in blocking solution. Cells were observed under a fluorescent microscope and images were acquired using DP Controller (OLYMPUS, Version 3.2.1.276). Mean fluorescence was measured using Image J (Version 1.49) and calculated using a formula previously described<sup>63</sup>.

**Differential staining of bone marrow derived cells.** Cells obtained from big brown bats bone marrow were concentrated onto a slide using Cytospin 4 (ThermoFisher). The slides were fixed in Hema 3 fixative solution (Fisher Scientific, USA) for 10 seconds, followed by 5 dips for 1 second each in Hema 3 solution I (Fisher Scientific, USA) then Hema 3 solution II (Fisher Scientific, USA). The slides were rinsed with deionized water, air dried and observed under a light microscope.

**Chromatin immunoprecipitation assay (ChIP).** HEK293T cells were seeded in 6-well plates at a concentration of  $3 \times 10^5$  cells/well. Cells at 60–70% confluency were co-transfected with the TNF $\alpha$  promoters and big brown bat c-Rel using Lipofectamine 2000 in serum free medium (OPTI-MEM, Gibco). After 4 h, serum free medium was replaced with complete medium and the cells were incubated for 16 h. After 16 h, cells were transfected with 750 ng/ml poly(I:C) and incubated for 4 h. The cells were then fixed using 1% formaldehyde (Thermo



Scientific) and processed for ChIP assay as per manufacturer's instructions (Pierce Agarose ChIP kit, Thermo Scientific). For immunoprecipitating HA-tagged big brown bat c-Rel, 1/1000 dilution of mouse anti-HA antibody (Sigma) was used and 5 µg mouse IgG isotype control (Thermo Scientific) was used as the non-specific antibody control. ChIP assay positive (human anti-RNA polymerase II) and negative control (rabbit IgG) antibodies were provided with the kit. Positive control primers for human GAPDH were provided with the kit. The amount of TNF $\alpha$  promoter immunoprecipitated was quantified by quantitative real-time PCR (qRT-PCR) and percent input was calculated and plotted as per manufacturer's instructions and as previously mentioned<sup>64</sup>. The qRT-PCR products were analysed by gel electrophoresis.

**Statistics.** Significance of the data was determined by two-tailed Mann Whitney *U* test for non-parametric independent samples using IBM SPSS (Version 21). In the figures, \**P* < 0.05 and \*\**P* < 0.01. Actual 'P values' are mentioned in figure legends.

## References

- Li, W. *et al.* Bats are natural reservoirs of SARS-like coronaviruses. *Science* **310**, 676–679, doi:10.1126/science.1118391 (2005).
- Memish, Z. A. *et al.* Middle East respiratory syndrome coronavirus in bats, Saudi Arabia. *Emerg Infect Dis* **19**, 1819–1823, doi:10.3201/eid1911.131172 (2013).
- Huang, Y. W. *et al.* Origin, evolution, and genotyping of emergent porcine epidemic diarrhea virus strains in the United States. *MBio* **4**, e00737–00713, doi:10.1128/mBio.00737-13 (2013).
- Moratelli, R. & Calisher, C. H. Bats and zoonotic viruses: can we confidently link bats with emerging deadly viruses? *Mem Inst Oswaldo Cruz* **110**, 1–22, doi:10.1590/0074-02760150048 (2015).
- Schountz, T. Immunology of Bats and Their Viruses: Challenges and Opportunities. *Viruses* **6**, 4880–4901, doi:10.3390/v6124880 (2014).
- O'Shea, T. J. *et al.* Bat flight and zoonotic viruses. *Emerg Infect Dis* **20**, 741–745, doi:10.3201/eid2005.130539 (2014).
- Middleton, D. J. *et al.* Experimental Nipah virus infection in pteropid bats (*Pteropus poliocephalus*). *J Comp Pathol* **136**, 266–272, doi:10.1016/j.jcpa.2007.03.002 (2007).
- Williamson, M. M. *et al.* Transmission studies of Hendra virus (equine morbilli-virus) in fruit bats, horses and cats. *Australian Veterinary Journal* **76**, 813–818, doi:10.1111/j.1751-0813.1998.tb12335.x (1998).
- Munster, V. J. *et al.* Replication and shedding of MERS-CoV in Jamaican fruit bats (*Artibeus jamaicensis*). *Sci Rep* **6**, 21878, doi:10.1038/srep21878 (2016).
- Paweska, J. T. *et al.* Experimental Inoculation of Egyptian Fruit Bats (*Rousettus aegyptiacus*) with Ebola Virus. *Viruses* **8**, 29, doi:10.3390/v8020029 (2016).
- Parkin, J. & Cohen, B. An overview of the immune system. *The Lancet* **357**, 1777–1789, doi:10.1016/s0140-6736(00)04904-7 (2001).
- Borghesi, L. & Milcarek, C. Innate versus adaptive immunity: a paradigm past its prime? *Cancer Res* **67**, 3989–3993, doi:10.1158/0008-5472.CAN-07-0182 (2007).
- Iwasaki, A. & Medzhitov, R. Toll-like receptor control of the adaptive immune responses. *Nat Immunol* **5**, 987–995, doi:10.1038/ni1112 (2004).
- Mogensen, T. H. Pathogen recognition and inflammatory signaling in innate immune defenses. *Clin Microbiol Rev* **22**, 240–273, Table of Contents, doi:10.1128/CMR.00046-08 (2009).
- Lee, M. S. & Kim, Y. J. Signaling pathways downstream of pattern-recognition receptors and their cross talk. *Annu Rev Biochem* **76**, 447–480, doi:10.1146/annurev.biochem.76.060605.122847 (2007).
- Koyama, S., Ishii, K. J., Coban, C. & Akira, S. Innate immune response to viral infection. *Cytokine* **43**, 336–341, doi:10.1016/j.cyt.2008.07.009 (2008).
- Kawai, T. & Akira, S. Innate immune recognition of viral infection. *Nat Immunol* **7**, 131–137, doi:10.1038/ni1303 (2006).
- Hoesel, B. & Schmid, J. A. The complexity of NF-kappaB signaling in inflammation and cancer. *Mol Cancer* **12**, 86, doi:10.1186/1476-4598-12-86 (2013).
- Kunsch, C., Ruben, S. M. & Rosen, C. A. Selection of Optimal kB/Rel DNA-Binding Motifs: Interaction of Both Subunits of NF-kB with DNA Is Required for Transcriptional Activation. *Molecular and Cellular Biology* **12**, 4412–4421, doi:10.1128/MCB.12.10.4412 (1992).
- Papenfuss, A. T. *et al.* The immune gene repertoire of an important viral reservoir, the Australian black flying fox. *BMC Genomics* **13**, 261, doi:10.1186/1471-2164-13-261 (2012).
- Cowled, C. *et al.* Molecular characterisation of Toll-like receptors in the black flying fox *Pteropus alecto*. *Dev Comp Immunol* **35**, 7–18, doi:10.1016/j.dci.2010.07.006 (2011).
- Cowled, C., Baker, M. L., Zhou, P., Tachedjian, M. & Wang, L. F. Molecular characterisation of RIG-I-like helicases in the black flying fox, *Pteropus alecto*. *Dev Comp Immunol* **36**, 657–664, doi:10.1016/j.dci.2011.11.008 (2012).
- Zhou, P. *et al.* IRF7 in the Australian black flying fox, *Pteropus alecto*: evidence for a unique expression pattern and functional conservation. *PLoS One* **9**, e103875, doi:10.1371/journal.pone.0103875 (2014).
- Zhou, P. *et al.* Type III IFNs in pteropid bats: differential expression patterns provide evidence for distinct roles in antiviral immunity. *J Immunol* **186**, 3138–3147, doi:10.4049/jimmunol.1003115 (2011).
- Zhou, P. *et al.* Type III IFN receptor expression and functional characterisation in the pteropid bat, *Pteropus alecto*. *PLoS One* **6**, e25385, doi:10.1371/journal.pone.0025385 (2011).
- Zhou, P., Cowled, C., Wang, L. F. & Baker, M. L. Bat Mx1 and Oas1, but not Pkr are highly induced by bat interferon and viral infection. *Dev Comp Immunol* **40**, 240–247, doi:10.1016/j.dci.2013.03.006 (2013).
- Zhou, P. *et al.* Contraction of the type I IFN locus and unusual constitutive expression of IFN- $\alpha$  in bats. *Proc Natl Acad Sci USA* **113**, 2696–2701, doi:10.1073/pnas.1518240113 (2016).
- Baker, M. L., Tachedjian, M. & Wang, L. F. Immunoglobulin heavy chain diversity in Pteropid bats: evidence for a diverse and highly specific antigen binding repertoire. *Immunogenetics* **62**, 173–184, doi:10.1007/s00251-010-0425-4 (2010).
- Wynne, J. W. *et al.* Purification and characterisation of immunoglobulins from the Australian black flying fox (*Pteropus alecto*) using anti-fab affinity chromatography reveals the low abundance of IgA. *PLoS One* **8**, e52930, doi:10.1371/journal.pone.0052930 (2013).
- Cowled, C. *et al.* Characterisation of novel microRNAs in the Black flying fox (*Pteropus alecto*) by deep sequencing. *BMC Genomics* **15**, 682, doi:10.1186/1471-2164-15-682 (2014).
- Gu, J. & Korteweg, C. Pathology and pathogenesis of severe acute respiratory syndrome. *Am J Pathol* **170**, 1136–1147, doi:10.2353/ajpath.2007.061088 (2007).
- Lau, S. K. *et al.* Delayed induction of proinflammatory cytokines and suppression of innate antiviral response by the novel Middle East respiratory syndrome coronavirus: implications for pathogenesis and treatment. *J Gen Virol* **94**, 2679–2690, doi:10.1099/vir.0.055533-0 (2013).
- Xu, X. *et al.* Porcine epidemic diarrhea virus E protein causes endoplasmic reticulum stress and up-regulates interleukin-8 expression. *Virol J* **10**, 26, doi:10.1186/1743-422X-10-26 (2013).



34. Tisoncik, J. R. *et al.* Into the eye of the cytokine storm. *Microbiol Mol Biol Rev* **76**, 16–32, doi:10.1128/MMBR.05015-11 (2012).
35. Banerjee, A. *et al.* Generation and Characterization of Eptesicus fuscus (Big brown bat) kidney cell lines immortalized using the Myotis polyomavirus large T-antigen. *J Virol Methods* **237**, 166–173, doi:10.1016/j.jviromet.2016.09.008 (2016).
36. Fu, T. *et al.* c-Rel is a transcriptional repressor of EPHB2 in colorectal cancer. *J Pathol* **219**, 103–113, doi:10.1002/path.2590 (2009).
37. Liou, H. C. & Hsia, C. Y. Distinctions between c-Rel and other NF-kappaB proteins in immunity and disease. *Bioessays* **25**, 767–780, doi:10.1002/bies.10306 (2003).
38. Ubalee, R. *et al.* Strong association of a tumor necrosis factor-alpha promoter allele with cerebral malaria in Myanmar. *Tissue Antigens* **58**, 407–410, doi:10.1034/j.1399-0039.2001.580610.x (2001).
39. Messeguer, X. *et al.* PROMO: detection of known transcription regulatory elements using species-tailored searches. *Bioinformatics* **18**, 333–334, doi:10.1093/bioinformatics/18.2.333 (2002).
40. Donaldson, E. F. *et al.* Metagenomic analysis of the viromes of three North American bat species: viral diversity among different bat species that share a common habitat. *J Virol* **84**, 13004–13018, doi:10.1128/JVI.01255-10 (2010).
41. Baker, M. L., Schountz, T. & Wang, L. F. Antiviral immune responses of bats: a review. *Zoonoses Public Health* **60**, 104–116, doi:10.1111/j.1863-2378.2012.01528.x (2013).
42. Rodhain, F. Bats and Viruses: complex relationships. *Bull Soc Pathol Exot* **108**, 272–289, doi:10.1007/s13149-015-0448-z (2015).
43. Ahn, M., Cui, J., Irving, A. T. & Wang, L. F. Unique Loss of the PYHIN Gene Family in Bats Amongst Mammals: Implications for Inflammation Sensing. *Sci Rep* **6**, 21722, doi:10.1038/srep21722 (2016).
44. McBride, R., van Zyl, M. & Fielding, B. C. The coronavirus nucleocapsid is a multifunctional protein. *Viruses* **6**, 2991–3018, doi:10.3390/v6082991 (2014).
45. Lu, X., Pan, J., Tao, J. & Guo, D. SARS-CoV nucleocapsid protein antagonizes IFN-beta response by targeting initial step of IFN-beta induction pathway, and its C-terminal region is critical for the antagonism. *Virus Genes* **42**, 37–45, doi:10.1007/s11262-010-0544-x (2011).
46. He, X. *et al.* Anti-lyssaviral activity of interferons kappa and omega from the serotine bat, Eptesicus serotinus. *J Virol* **88**, 5444–5454, doi:10.1128/JVI.03403-13 (2014).
47. He, X. *et al.* Establishment of Myotis myotis Cell Lines - Model for Investigation of Host-Pathogen Interaction in a Natural Host for Emerging Viruses. *PLoS One* **9**, e109795, doi:10.1371/journal.pone.0109795 (2014).
48. Omatsu, T. *et al.* Induction and sequencing of Roussette bat interferon alpha and beta genes. *Vet Immunol Immunopathol* **124**, 169–176, doi:10.1016/j.vetimm.2008.03.004 (2008).
49. Martinez Gomez, J. M. *et al.* Phenotypic and functional characterization of the major lymphocyte populations in the fruit-eating bat Pteropus alecto. *Sci Rep* **6**, 37796, doi:10.1038/srep37796 (2016).
50. Zhou, P. *et al.* Unlocking bat immunology: establishment of Pteropus alecto bone marrow-derived dendritic cells and macrophages. *Sci Rep* **6**, 38597, doi:10.1038/srep38597 (2016).
51. Zhou, Y. *et al.* TLR3 activation efficiency by high or low molecular mass poly I:C. *Innate Immun* **19**, 184–192, doi:10.1177/1753425912459975 (2013).
52. Bradley, J. R. TNF-mediated inflammatory disease. *J Pathol* **214**, 149–160, doi:10.1002/path.2287 (2008).
53. Rothwarf, D. M. & Karin, M. The NF-kappa B activation pathway: a paradigm in information transfer from membrane to nucleus. *Sci STKE* **1999**, RE1, doi:10.1126/stke.1999.5.re1 (1999).
54. Zhang, G. *et al.* Comparative analysis of bat genomes provides insight into the evolution of flight and immunity. *Science* **339**, 456–460, doi:10.1126/science.1230835 (2013).
55. Enchery, F. & Horvat, B. Understanding the interaction between henipaviruses and their natural host, fruit bats: Paving the way toward control of highly lethal infection in humans. *Int Rev Immunol*, 1–14, doi:10.1080/08830185.2016.1255883 (2017).
56. Madaan, A., Verma, R., Singh, A. T., Jain, S. K. & Jaggi, M. A stepwise procedure for isolation of murine bone marrow and generation of dendritic cells. *Journal of Biological Methods* **1**, doi:10.14440/jbm.2014.12 (2014).
57. Rapin, N. *et al.* Activation of Innate Immune-Response Genes in Little Brown Bats (Myotis lucifugus) Infected with the Fungus Pseudogymnoascus destructans. *PLoS One* **9**, e112285, doi:10.1371/journal.pone.0112285 (2014).
58. Wang, X. A. PCR primer bank for quantitative gene expression analysis. *Nucleic Acids Research* **31**, 154e–154, doi:10.1093/nar/gng154 (2003).
59. Wang, X., Spandidos, A., Wang, H. & Seed, B. PrimerBank: a PCR primer database for quantitative gene expression analysis, 2012 update. *Nucleic Acids Res* **40**, D1144–1149, doi:10.1093/nar/gkr1013 (2012).
60. Wang, W. & Malcolm, B. A. Two-stage PCR protocol allowing introduction of multiple mutations, deletions and insertions using QuikChange Site-Directed Mutagenesis. *Biotechniques* **26**, 680–682 (1999).
61. Bodnarchuk, T. W., Napper, S., Rapin, N. & Misra, V. Mechanism for the induction of cell death in ONS-76 medulloblastoma cells by Zhangfei/CREB-ZF. *J Neurooncol* **109**, 485–501, doi:10.1007/s11060-012-0927-z (2012).
62. Smith, F. D. *et al.* AKAP-Lbc enhances cyclic AMP control of the ERK1/2 cascade. *Nat Cell Biol* **12**, 1242–1249, doi:10.1038/ncb2130 (2010).
63. McCloy, R. A. *et al.* Partial inhibition of Cdk1 in G2 phase overrides the SAC and decouples mitotic events. *Cell Cycle* **13**, 1400–1412, doi:10.4161/cc.28401 (2014).
64. Haring, M. *et al.* Chromatin immunoprecipitation: optimization, quantitative analysis and data normalization. *Plant Methods* **3**, 11, doi:10.1186/1746-4811-3-11 (2007).

## Acknowledgements

Funding for the research was obtained from a Natural Sciences and Engineering Research Council of Canada (NSERC) Discovery grant awarded to Vikram Misra and Integrated Training Program in Infectious Disease, Food Safety and Public Policy (ITraP) funded by NSERC/CREATE. Arinjay Banerjee was funded by ITraP, Saskatchewan Innovation and Opportunity Scholarship and the Department of Veterinary Microbiology, University of Saskatchewan. We would also like to thank the Canadian Wildlife Health Cooperative at the University of Saskatchewan for their support and expertise.

## Author Contributions

A.B. and N.R. performed the experiments; T.B. provided materials; A.B., T.B. and V.M. provided intellectual inputs; V.M. supervised the study; A.B., N.R., T.B. and V.M. wrote the manuscript; All authors reviewed the manuscript.

## Additional Information

**Supplementary information** accompanies this paper at doi:10.1038/s41598-017-01513-w

**Competing Interests:** The authors declare that they have no competing interests.

**Publisher's note:** Springer Nature remains neutral with regard to jurisdictional claims in published maps and institutional affiliations.



**Open Access** This article is licensed under a Creative Commons Attribution 4.0 International License, which permits use, sharing, adaptation, distribution and reproduction in any medium or format, as long as you give appropriate credit to the original author(s) and the source, provide a link to the Creative Commons license, and indicate if changes were made. The images or other third party material in this article are included in the article's Creative Commons license, unless indicated otherwise in a credit line to the material. If material is not included in the article's Creative Commons license and your intended use is not permitted by statutory regulation or exceeds the permitted use, you will need to obtain permission directly from the copyright holder. To view a copy of this license, visit <http://creativecommons.org/licenses/by/4.0/>.

© The Author(s) 2017